Wireless Power Supply for Small Household Appliances Using Energy Model

XUJIAN SHU, WENXUN XIAO[ID], (Member, IEEE), AND BO ZHANG[ID], (Senior Member, IEEE)

School of Electric Power, South China University of Technology, Guangzhou 510641, China

Corresponding author: Bo Zhang (epbzhang@scut.edu.cn)

ABSTRACT In order to resolve the safety and stability of the power supply for household appliances, a system of wireless power supply for household appliances with Bluetooth communication based on electromagnetic resonance is proposed. In this paper, the energy model of wireless power transfer system is first proposed, which is based on the circuit equations and variable substitution, more accurate than the coupled-mode model and simpler than the circuit model. Then, the characteristics of output power and transfer efficiency of the wireless power transfer system are analyzed, and a system of wireless power supply for small household appliances has been designed and implemented. Furthermore, Bluetooth communication is applied to achieve various protection functions of the system, therefore enhancing the safety and stability of the system. Experimental results show that this power supply system achieves a stable output dc voltage of 48 V and a large output power of 100 W, the total efficiency is more than 80% within a distance of 30 cm.

INDEX TERMS Household appliances, wireless power transfer, energy model.

I. INTRODUCTION

With the rapid development of science and technology, and the continuous improvement of people's living standards, people gradually realize that there are many shortcomings in the traditional wire-based power transfer method. Firstly, the wear, aging and corrosion of the wires may lead to electric leakage accidents, which may burn out the electric appliances or even cause power system failures, endangering people's safety [1]. Secondly, with the continuous enrichment of household appliances and daily electronic products, various kinds of power cords and outlets have caused unnecessary troubles for people's lives and reduce the convenience of people's lives [2]. Therefore, to avoid the above shortages of the wire-based power transfer method, the wireless power transfer (WPT) technology has gradually attracted extensive attention, based on the security, convenience and reliability of this technology, increasing number of products with the function of wireless charging widely enter into people's lives.

In 2009, Dell introduced a wireless-powered laptop, namely Latitude Z, that combines WPT technology with the power of the laptop, the time required for charging saturation is as good as the standard charger [3]. In 2010, Haier demonstrated the world's first no-tail TV at the 43rd International Consumer Electronic Show (CES), which was developed by Haier and the Massachusetts Institute of Technology, and realized wireless power supply based on magnetic coupling

resonance [4], [5]. In the same year, Haier cooperated with Chongqing university to develop an inductively coupled wireless power supply system for kitchen appliances (blender, rice cooker and others) by using the principle of electromagnetic induction coupling. Then in 2012, Haier launched the world's first no-tail kitchen electricity at the International Funkausstellung Berlin (IFA), which opened a new chapter in the future of kitchen appliances [6]. In 2013, the Toshiba unveiled an OLED lighting panel supporting wireless power transfer at Tokyo Lighting Fair [7]. In recent years, the products based on wireless power supply have emerged in an endless stream, and wireless power supply for household appliances has received more and more attention.

However, the wireless power supply technology of household appliances is still not mature enough, and there has been a lot of efforts on how to improve the power and the transfer efficiency, and to introduce flexibility to application. In [2], a small-scale resonant coupling prototype is designed and the transfer efficiency goes up to 75%, but when the distance exceeds 10cm, the efficiency drops to less than 50%, which is an obvious restriction for application. In [8], a dipole coil design is presented to improve the efficiency and they successfully transferred 150W power, however there must be a reflector either beside the transmitting coil or beside the receiving coil, thus the structure is too complicated for home use. Also, Kim *et al.* [9] are working on using an intermediate
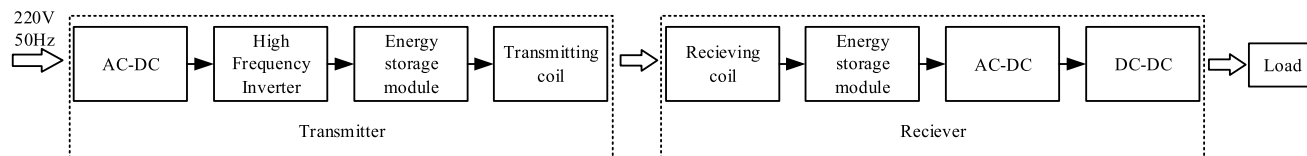
FIGURE 1. Block diagram of the system of wireless power supply for small household appliances.
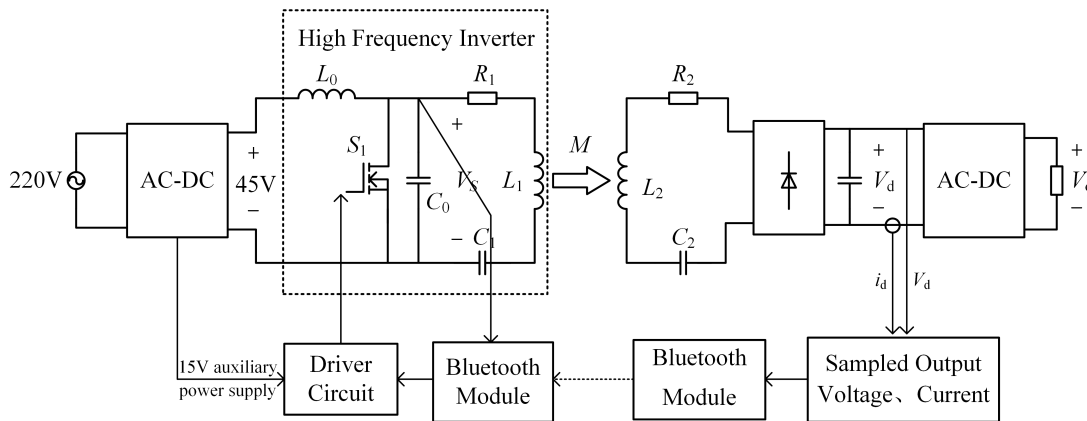

FIGURE 2. Detailed circuit diagram of the system of wireless power supply for small household appliances.

resonant coil of two loops to enhance energy transfer to power a TV, however the transferring efficiency is only 72.85% and the intermediate coil is causing too much energy lost and complexity. Reference [10] expresses the design of a WPT system with multiple self-resonators for an LED TV and exhibits the transfer efficiency of 80%. But it has the same problem on system structure which cause too much trouble on usability.

Therefore, in this paper, a system of wireless power supply for small household appliances based on electromagnetic resonance with a power of about 100W is proposed and designed. Firstly, based on circuit theory, the energy model of the system is established, and the characteristics of output power and transfer efficiency are analyzed. Then, the experimental prototype of the system is built, to better understand the characteristics of the system, we tested the total efficiency and output power within a distance of 25cm to 45cm, and found that the total efficiency within 30cm is more than 80%, which satisfies the demand of household appliances with high system efficiency. Moreover, the control strategy based on Bluetooth is further proposed to realize wireless communication of WPT system, which ensures the stability of output voltage and power, improves the reliability and efficiency of the system, greatly reduces the load loss and achieves various protection of no-load, overvoltage, overcurrent and close distance, which improves the security and reliability of the system.

II. SYSTEM STRUCTURE

The system of wireless power supply for small household appliances mainly contains transmitter module, receiver module, and load (that is small household appliance), the block diagram of the whole power supply system is shown in Fig. 1. The transmitter module transmits electric energy to receiver module through air based on the principle of electromagnetic resonance, then the receiver module provides power for household appliances. The detailed circuit diagram of the system is shown in Fig. 2.

As illustrated in Fig. 2, The transmitter module includes a rectifier to provide 45V dc power supply for class-E high-frequency inverter that generates 1 MHz sinusoidal current, a transmitting coil, a series capacitor for making up a resonator with transmitting coil and Bluetooth module to receive feedback from receiver module, the receiver module comprises a receiving coil, a series capacitor to make up a resonator with receiving coil, an uncontrolled rectifier, a DC-DC converter to control the output power and Bluetooth module to feed the load information to transmitter module in real time, the load refers to small household appliances. Specifically, the Bluetooth communication module is applied to ensure the stable operation of the system so as to improve the efficiency in this paper.

III. ENERGY MODEL OF WPT SYSTEM

In general, the rectifier and class-E inverter are assumed to be a high frequency ac voltage source u_s, and the equivalent ac resistance is R_L. Thus, any WPT system can be simplified as a two-coil equivalent circuit, regardless of the number and structure of its coils, as shown in Fig. 3. The inductances of the transmitting coil and receiving coil are L_1 and L_2, the corresponding resonant capacitances and internal resistances are referred to as C_1, C_2, R_1 and R_2, the currents flowing through
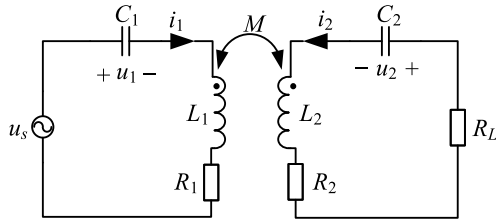
FIGURE 3. Simplified circuit of WPT system.

transmitting and receiving coil are i_1 and i_2, and the voltage across the resonant capacitances of the transmitter and receiver are u_1 and u_2. M is the mutual inductance between the transmitting and receiving coil.

According to the energy storage characteristics of inductors and capacitors, the total energy stored in the transmitter and receiver, W_1 and W_2, can be expressed as

$$\begin{cases} W_1 = \dfrac{1}{2}L_1 i_1^2 + \dfrac{1}{2}C_1 u_1^2 \\ W_2 = \dfrac{1}{2}L_2 i_2^2 + \dfrac{1}{2}C_2 u_2^2 \end{cases} \tag{1}$$

Defining the conjugate complex variable pairs of energy $e_{1\pm}$ and $e_{2\pm}$ as

$$\begin{cases} e_{1\pm} = \sqrt{\dfrac{L_1}{2}}i_1 \pm j\sqrt{\dfrac{C_1}{2}}u_1 \\ e_{2\pm} = \sqrt{\dfrac{L_2}{2}}i_2 \pm j\sqrt{\dfrac{C_2}{2}}u_2 \end{cases} \tag{2}$$

here, $|e_{1+}|^2 = |e_{1-}|^2 = e_{1+}e_{1-} = W_1$ and $|e_{2+}|^2 = |e_{2-}|^2 = e_{2+}e_{2-} = W_2$.

From (2), we can get the expressions of the voltage and current, u_1, u_2, i_1 and i_2 as

$$\begin{cases} i_m = \dfrac{1}{\sqrt{2L_m}}(e_{m+} + e_{m-}) \\ u_m = -j\dfrac{1}{\sqrt{2C_m}}(e_{m+} - e_{m-}) \end{cases} \tag{3}$$

where $m = 1$ or 2.

The voltage and current equations of the circuit in the Fig. 3 are

$$\begin{cases} u_s = u_1 + i_1 R_1 + L_1 \dfrac{di_1}{dt} + M\dfrac{di_2}{dt} \\ i_1 = C_1 \dfrac{du_1}{dt} \\ 0 = u_2 + i_2 (R_2 + R_L) + L_2 \dfrac{di_2}{dt} + M\dfrac{di_1}{dt} \\ i_2 = C_2 \dfrac{du_2}{dt} \end{cases} \tag{4}$$

Substituting (3) into (4) to eliminate u_1, u_2, i_1 and i_2, we can obtain the energy model of WPT system as

$$\frac{de_{1+}}{dt} = \left[j\omega_1 \frac{2-k^2}{2(1-k^2)} - \frac{R_1}{2L_1(1-k^2)} \right]e_{1+}$$

$$+ \left[-j\frac{\omega_2 k}{2(1-k^2)} + \frac{k(R_2+R_L)}{2L_2(1-k^2)} \right]e_{2+}$$

$$+ \frac{1}{(1-k^2)}\sqrt{\frac{1}{2L_1}}u_s$$

$$+ \left[-j\omega_1 \frac{k^2}{2(1-k^2)} - \frac{R_1}{2L_1(1-k^2)} \right]e_{1-}$$

$$+ \left[j\frac{\omega_2 k}{2(1-k^2)} + \frac{k(R_2+R_L)}{2L_2(1-k^2)} \right]e_{2-} \tag{5a}$$

$$\frac{de_{1-}}{dt} = \left[-j\omega_1 \frac{2-k^2}{2(1-k^2)} - \frac{R_1}{2L_1(1-k^2)} \right]e_{1-}$$

$$+ \left[j\frac{\omega_2 k}{2(1-k^2)} + \frac{k(R_2+R_L)}{2L_2(1-k^2)} \right]e_{2-}$$

$$+ \frac{1}{(1-k^2)}\sqrt{\frac{1}{2L_1}}u_s$$

$$+ \left[j\omega_1 \frac{k^2}{2(1-k^2)} - \frac{R_1}{2L_1(1-k^2)} \right]e_{1+}$$

$$+ \left[-j\frac{\omega_2 k}{2(1-k^2)} + \frac{k(R_2+R_L)}{2L_2(1-k^2)} \right]e_{2+} \tag{5b}$$

$$\frac{de_{2+}}{dt} = \left[-j\frac{\omega_1 k}{2(1-k^2)} + \frac{kR_1}{2L_1(1-k^2)} \right]e_{1+}$$

$$+ \left[j\omega_2 \frac{2-k^2}{2(1-k^2)} - \frac{(R_2+R_L)}{2L_2(1-k^2)} \right]e_{2+}$$

$$- \frac{k}{(1-k^2)}\sqrt{\frac{1}{2L_1}}u_s$$

$$+ \left[j\frac{\omega_1 k}{2(1-k^2)} + \frac{kR_1}{2L_1(1-k^2)} \right]e_{1-}$$

$$+ \left[-j\omega_2 \frac{k^2}{2(1-k^2)} - \frac{(R_2+R_L)}{2L_2(1-k^2)} \right]e_{2-} \tag{5c}$$

$$\frac{de_{2-}}{dt} = \left[j\frac{\omega_1 k}{2(1-k^2)} + \frac{kR_1}{2L_1(1-k^2)} \right]e_{1-}$$

$$+ \left[-j\omega_2 \frac{2-k^2}{2(1-k^2)} - \frac{(R_2+R_L)}{2L_2(1-k^2)} \right]e_{2-}$$

$$- \frac{k}{(1-k^2)}\sqrt{\frac{1}{2L_1}}u_s$$

$$+ \left[-j\frac{\omega_1 k}{2(1-k^2)} + \frac{kR_1}{2L_1(1-k^2)} \right]e_{1+}$$

$$+ \left[j\omega_2 \frac{k^2}{2(1-k^2)} - \frac{(R_2+R_L)}{2L_2(1-k^2)} \right]e_{2+} \tag{5d}$$

here, $k = M/\sqrt{L_1 L_2}$ is coupling coefficient, $\omega_1 = 1/\sqrt{L_1 C_1}$ and $\omega_2 = 1/\sqrt{L_2 C_2}$ are natural frequencies of transmitting and receiving coil, respectively.

Since e_{1+} (e_{2+}) and e_{1-} (e_{2-}) are complex conjugate pairs, they can be represented by counter-rotating vectors, the

normal modes e_{1+} (e_{2+}) will be little affected by the complex conjugate modes e_{1-} (e_{2-}). Neglecting the coupling terms between normal modes e_{1+} (e_{2+}) and complex conjugate modes e_{1-} (e_{2-}), (5) can be reduced to

$$
\begin{cases}
\dfrac{de_{1+}}{dt} = \left[j\omega_1 \dfrac{2-k^2}{2\left(1-k^2\right)} - \dfrac{\tau_1}{\left(1-k^2\right)} \right] e_{1+} \\
\quad + \left[-j\dfrac{\omega_2 k}{2\left(1-k^2\right)} + \dfrac{k\tau_{2L}}{\left(1-k^2\right)} \right] e_{2+} \\
\quad + \dfrac{1}{\left(1-k^2\right)} \sqrt{\dfrac{1}{2L_1}} u_s \\
\dfrac{de_{2+}}{dt} = \left[-j\dfrac{\omega_1 k}{2\left(1-k^2\right)} + \dfrac{k\tau_1}{\left(1-k^2\right)} \right] e_{1+} \\
\quad + \left[j\omega_2 \dfrac{2-k^2}{2\left(1-k^2\right)} - \dfrac{\tau_{2L}}{\left(1-k^2\right)} \right] e_{2+} \\
\quad - \dfrac{k}{\left(1-k^2\right)} \sqrt{\dfrac{1}{2L_1}} u_s
\end{cases}
\tag{6}
$$

where $\tau_1 = R_1/2L_1$, $\tau_2 = R_2/2L_2$, $\tau_L = R_L/2L_2$ and $\tau_{2L} = \tau_2 + \tau_L$.

According to (6), the energy transfer waveforms of the two coils without the load and with the load can be obtained as shown in Fig. 4(a) and Fig. 4(b), in which all energy variables are divided by W_1 for normalization.

From Fig. 4, it can be found that when all the initial energy is stored in the transmitting coil, as time evolves, the energy is exchanged back and forth between the transmitting and receiving coil, and eventually the energy oscillatory damps to zero, the damping ration is related to the internal resistances and load resistance of the system.

Considering all quantities oscillate as $e^{j\omega t}$, the solution of (6) can be represented as
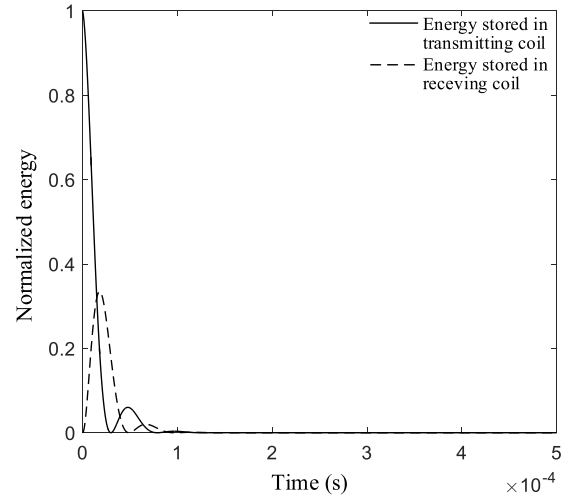
$$
\begin{cases}
e_{1+} \\
\quad = \dfrac{\left[j\left(\omega-\omega_2\right) + \tau_2 + \tau_L \right] \dfrac{1}{\left(1-k^2\right)} \sqrt{\dfrac{1}{2L_1}} U_s e^{j\omega t}}{\left\{ \begin{array}{l} -\left[\omega-\omega_1\dfrac{2-k^2}{2\left(1-k^2\right)}\right]\left[\omega-\omega_2\dfrac{2-k^2}{2\left(1-k^2\right)}\right] + \dfrac{\omega_1\omega_2 k^2}{4\left(1-k^2\right)^2} \\ + \dfrac{\tau_1\left(\tau_2+\tau_L\right)}{\left(1-k^2\right)} + j\dfrac{\left(\omega-\omega_1\right)\left(\tau_2+\tau_L\right) + \left(\omega-\omega_2\right)\tau_1}{\left(1-k^2\right)} \end{array} \right\}} \\
e_{2+} \\
\quad = \dfrac{-j\left(\omega-\frac{1}{2}\omega_1\right) \dfrac{k}{\left(1-k^2\right)} \sqrt{\dfrac{1}{2L_1}} U_s e^{j\omega t}}{\left\{ \begin{array}{l} -\left[\omega-\omega_1\dfrac{2-k^2}{2\left(1-k^2\right)}\right]\left[\omega-\omega_2\dfrac{2-k^2}{2\left(1-k^2\right)}\right] + \dfrac{\omega_1\omega_2 k^2}{4\left(1-k^2\right)^2} \\ + \dfrac{\tau_1\left(\tau_2+\tau_L\right)}{\left(1-k^2\right)} + j\dfrac{\left(\omega-\omega_1\right)\left(\tau_2+\tau_L\right) + \left(\omega-\omega_2\right)\tau_1}{\left(1-k^2\right)} \end{array} \right\}}
\end{cases}
\tag{7}
$$

The power delivered to the load can be described as

$$
P_L = 2\tau_L \left| e_{2+} \right|^2
$$
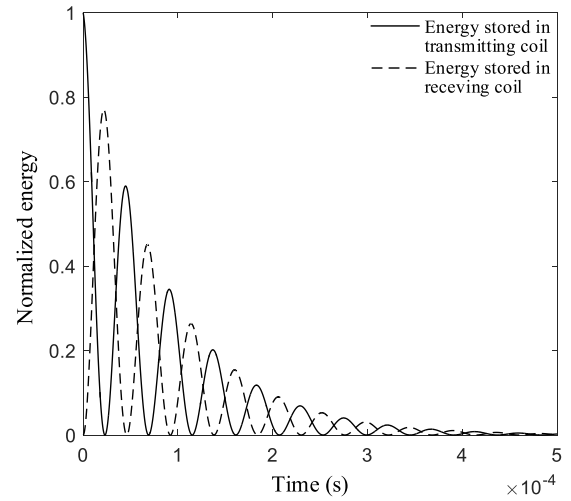
(a)

(b)

FIGURE 4. Energy exchange waveforms between the transmitting and receiving coil. (a) Considering internal resistances but no load. (b) Considering internal resistances and load.

$$
= \dfrac{\tau_L\left(\omega-\frac{1}{2}\omega_1\right)^2 \dfrac{k^2}{\left(1-k^2\right)^2} \dfrac{1}{L_1} U_s^2}{\left\langle \left\{ \begin{array}{l} -\left[\omega-\omega_1\dfrac{2-k^2}{2\left(1-k^2\right)}\right]\left[\omega-\omega_2\dfrac{2-k^2}{2\left(1-k^2\right)}\right] \\ + \dfrac{\omega_1\omega_2 k^2}{4\left(1-k^2\right)^2} + \dfrac{\tau_1\left(\tau_2+\tau_L\right)}{\left(1-k^2\right)} \end{array} \right\}^2 \\ + \dfrac{\left[\left(\omega-\omega_1\right)\left(\tau_2+\tau_L\right) + \left(\omega-\omega_2\right)\tau_1\right]^2}{\left(1-k^2\right)^2} \right\rangle}
\tag{8}
$$

and the transfer efficiency can be given as

$$
\eta = \dfrac{\tau_L \left| e_{2+} \right|^2}{\tau_1 \left| e_{1+} \right|^2 + \left(\tau_2+\tau_L\right) \left| e_{2+} \right|^2} \times 100\%
$$

$$
= \dfrac{\tau_L}{\tau_1 \dfrac{\left(\omega-\omega_2\right)^2 + \left(\tau_2+\tau_L\right)^2}{\left(\omega-\frac{1}{2}\omega_1\right)^2 k^2} + \tau_2 + \tau_L} \times 100\%
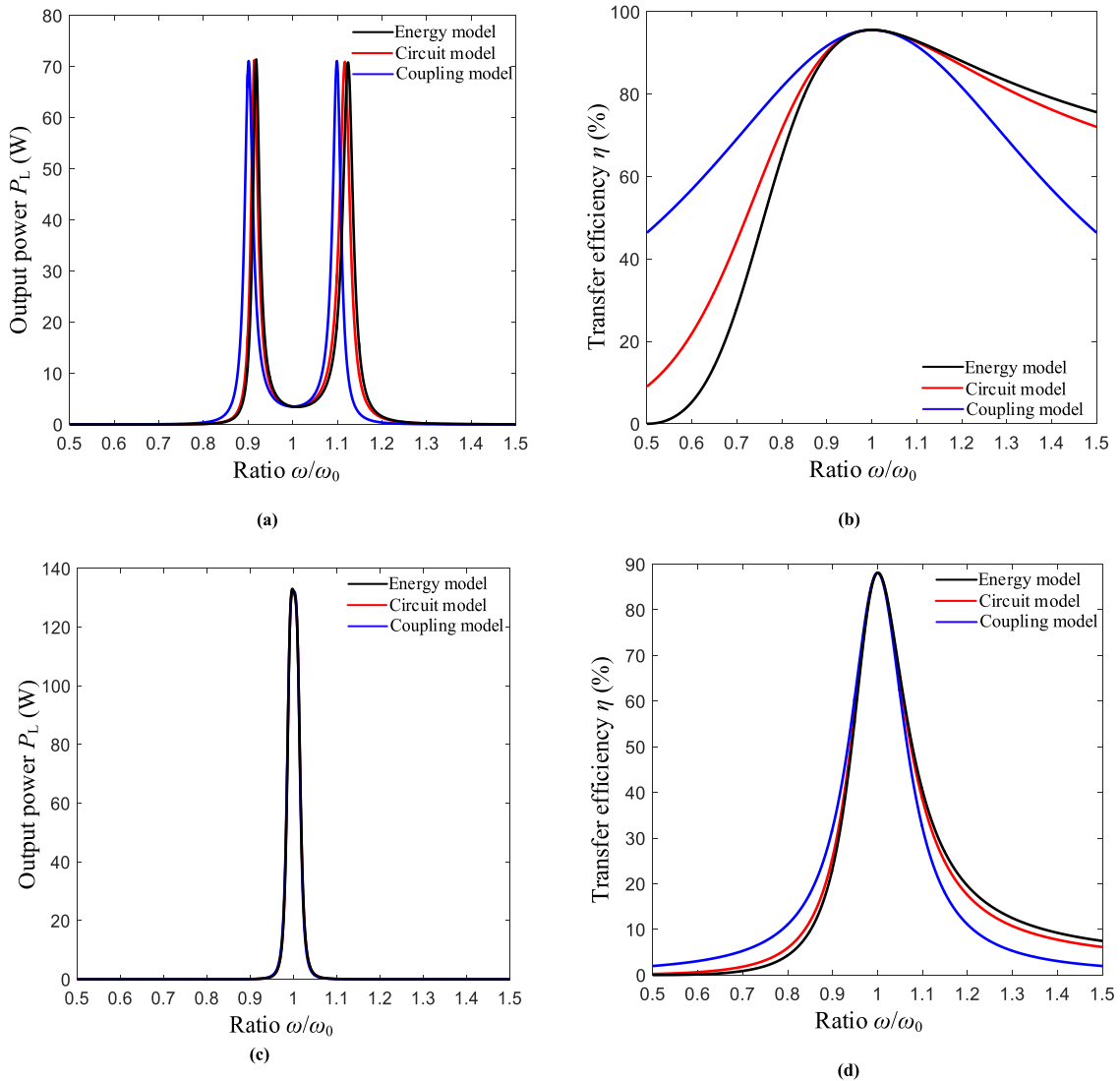\tag{9}
$$

FIGURE 5. Comparison of output power and transfer efficiency of three models as functions of operating frequency in strong and weak coupling region. (a) Comparison of output power of three models in strong coupling region $k = 0.2$. (b) Comparison of transfer efficiency of three models in strong coupling region $k = 0.2$. (c) Comparison of output power of three models in weak coupling region $k = 0.01$. (d) Comparison of transfer efficiency of three models in weak coupling region $k = 0.01$.

Comparing with output power and transfer efficiency of the circuit model and coupling model in the non-resonant state, as shown in Fig. 5, we can find that the energy model proposed is more accurate than the coupling model based on the coupled-mode theory in both strong and weak coupling cases when the system is in the non-resonant state [11]. Moreover, the energy model is simpler than the circuit model and directly reflect the energy exchange process between the transmitting and receiving coil. Thus, energy model is more applicable to the modeling of WPT system than the other two models.

From (8) and (9), we can find that the output power and transfer efficiency are optimal when the operating frequency ω of the system is equal to the natural resonant frequency $\omega_1 = \omega_2 = \omega_0$ of the coil in the weak-coupling region.

The optimal power delivered to load and optimal transfer efficiency can be expressed as

$$P_L = \frac{\frac{1}{4}\frac{\omega_0^2 k^2 \tau_L}{L_1} U_s^2}{\left[\frac{\omega_0^2 k^2}{4} + \tau_1(\tau_2 + \tau_L)\right]^2} \tag{10}$$

$$\eta = \frac{\tau_L}{\frac{4\tau_1(\tau_2+\tau_L)^2}{\omega_0^2 k^2} + \tau_2 + \tau_L} \times 100\% \tag{11}$$

Considering that when designing the system, it is expected that the transfer efficiency of the system can still reach more than 80% when the transfer distance is about 30cm, hence, according to (10) and (11), we can determine the optimal working interval of the system at a distance of about 30cm,
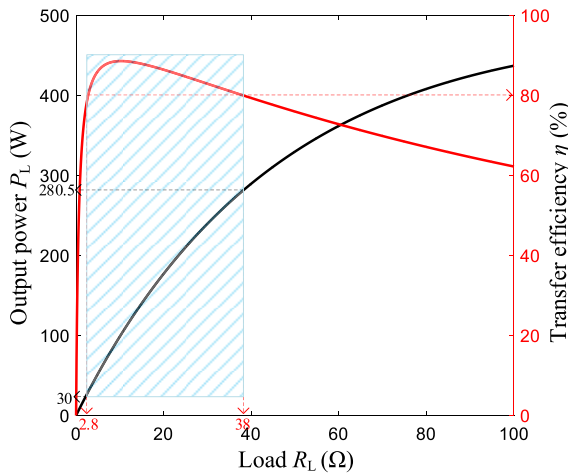
FIGURE 6. Output power and transfer efficiency of the system as a function of load resistance at a distance of about 30cm.

as shown in Fig. 6. From Fig.6, it can be seen that the optimal value of the load resistance is between 2.8Ω and 38Ω under the requirements of 30cm transfer distance and 80% transfer efficiency, which provides guidelines for parameter design of class-E inverter.

To understand the characteristics of the WPT system's output power and transfer efficiency varying with transfer distance and load resistance, the 3-D curved diagram of the power delivered to load and transfer efficiency varying with transfer distance and load resistance can be drawn as Fig. 7. According to Fig. 7, we can determine the optimal load, the power delivered to load and transfer efficiency under different loads and transfer distances, which laying the theoretical foundation for further design of circuit parameters.

IV. DESIGN AND IMPLEMENTATION OF SYSTEM

The design and implementation of the whole system mainly divide into several relatively important segments including coils, class-E high-frequency inverter, and Bluetooth communication module, as illuminated in Fig. 2.

A. COILS

Coils are the core components of WPT system to realize electromagnetic coupling resonance, and the power transfer efficiency and the power delivered to load are two key indicators to describe the performance of WPT system. Therefore, combing with (10) and (11), we can get

$$P_L = 2U_s^2 \cdot \frac{Q_1 Q_{2L}}{\omega_0 L_1 Q_L} \cdot \frac{k^2 Q_1 Q_{2L}}{\left(k^2 Q_1 Q_{2L} + 1\right)^2} \quad (12)$$

$$\eta = \frac{k^2 Q_1 Q_{2L}}{1 + k^2 Q_1 Q_{2L}} \cdot \frac{Q_{2L}}{Q_L} \times 100\% \quad (13)$$

Where $Q_1 = \omega L_1/R_1$ and $Q_2 = \omega L_2/R_2$ are the unloaded quality factor of transmitting coil and receiving coil, respectively. $Q_L = \omega L_2/R_L$ is the loaded quality factor, and $Q_L = \omega L_2/(R_2 + R_L) = Q_L Q_2/(Q_2 + Q_L)$.
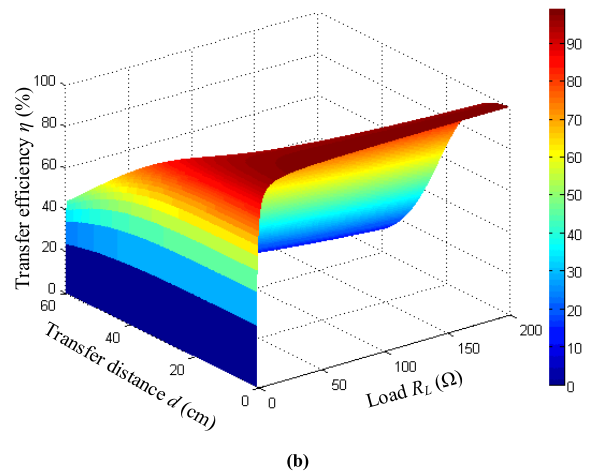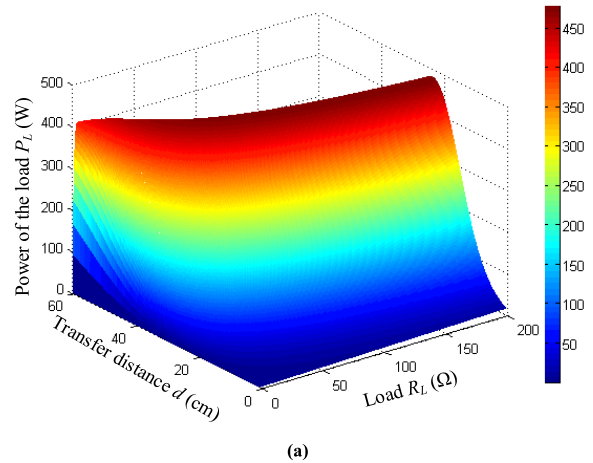

(a)

(b)

FIGURE 7. 3-D curved diagram of the power delivered to load P_L and transfer efficiency η varying with transfer distance d and load resistance R_L. (a) The load power P_L versus transfer distance d and load resistance R_L. (b) The transfer efficiency η versus transfer distance d and load resistance R_L.

According to (12) and (13), to obtain a high transfer efficiency, the coupling coefficient k and the quality factors of coils Q_1, Q_2 should be increased when designing the coils, which can be achieved by the size parameters of the coil.

The main parameters of the coils include the material of wire, diameter of wire w, radius of coil r, number of coil's turns N, turn spacing b and shape. Electrical conductivity and ac resistance of various material are different, the ac resistance reduces with the increase of wire diameter, but it will lead to large skin effect, resulting in an increase in loss. The selection of turn spacing is mainly to reduce the proximity effect thereby reducing loss. The radius of coil and coil turns can be determined by taking the quality factor of coils, magnetic field intensity and application into account. In our system, considering the size requirements of small household appliances such as refrigerator and washing machine, the cylindrical spiral coil with 2.5mm diameter of cooper wire, radius of 12.5cm, turns of 12, and turn spacing of 2mm, is chosen to generate a larger magnetic-filed intensity at a

distance of 30cm and a higher quality factor of coils. In the case that the size of coil is known, its electrical parameters such as inductance, resistance and quality factor of coil can be calculated [12].

B. CLASS-E HIGH-FREQUENCY INVERTER

Since the class-E high-frequency inverter can generate large currents at frequencies in the megahertz ranges and provide enough degrees of freedom to adapt the switch voltage to have both zero value and zero slope at switch turn on, which helps to decrease the losses, the class-E inverter was selected to produce a 1MHz sinusoidal current signal, its equivalent circuit diagram is shown in Fig. 2. According to Fig. 6, the optimal load is about 14Ω, thus, combining the conditions that the MOSFET works in an ideal state that both the value and the slope of switch voltage are zero at switch turn on, and the efficiency of class-E inverter is 100%, the parameters of class-E inverter can be determined [13], [14].

C. BLUETOOTH COMMUNICATION

In recent years, wireless data transmission technology is developing rapidly, the popular wireless data transmission mode has forms of Zigbee, Bluetooth and WiFi, which worked on the 2.4 GHz frequency band. In contrast to Zigbee and WiFi, the power consumption of Bluetooth is lowest, and it has satisfied the distance requirement of the WPT device, thus, Bluetooth communication is a good choice. In the actual operation of our system, empty and light-load failures occur occasionally, it will give rise to a large power loss that may cause a sharp rise in the temperature of the transmitter board to burn the MOSFET or tuning capacitors if the transmitter still works normally, and sometimes, the distance between transmitting and receiving coil decreases that makes larger coupling coefficient and reflected resistance so that the hard switching of class-E inverter occurs. In order to avoid above situations happening, feeding the data of receiver back to transmitter to control class-E inverter by wireless communication plays an important role in stable operation of system. Therefore, the design of Bluetooth communication module is crucial to the whole system.

As shown in Fig. 2, the Bluetooth communication module consists of two parts, the Bluetooth device in transmitter using slave role automatically enters into the working mode of close protection after power-on initialization, which uses the method of gradually increasing the input power to control the driving signal of switch as shown in Fig. 8(a), and receives feedback from receiver to control the class-E inverter to work at light-load hiccup mode, as shown in Fig. 8(b). The Bluetooth device in receiver works using the host role processes and sends the sampling information to transmitter. The entire control program is shown in Fig. 9. V_g is gate driving voltage signal of class-E inverter, V_d is the input dc voltage of DC-DC converter on the receiver.

In Fig. 8(a), T_1 is working time of switch, T_2 is break time of switch, $\triangle T$ is time step, at the first stage, switch intermittently works to complete the connection between Bluetooth
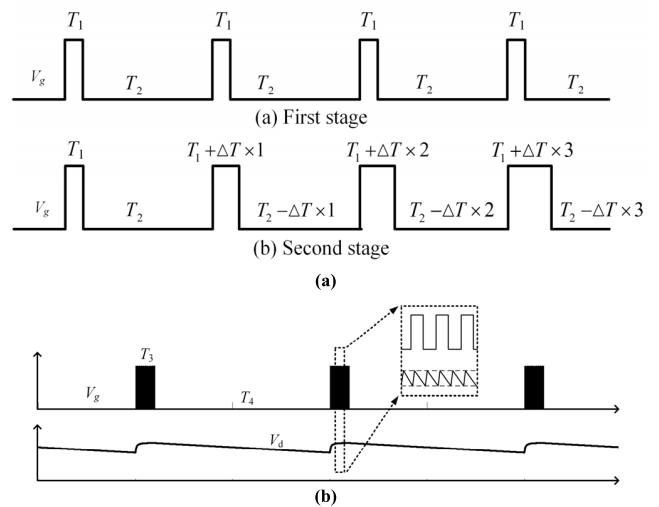

FIGURE 8. The waveforms of driving signal and output voltage. (a) The driving signal in two stages based on close protection. (b) The driving signal and output voltage based on light-load hiccup mode.

TABLE 1. Parameters of experiment circuit.

Symbol	Parameters	Values
w	Diameter of copper wire	2.5mm
r	Radius of coils	12.5cm
b	Turn spacing	2mm
N	Number of turns	12
L_1	Choke inductance	81μH
L_2	Inductance of transmitting coil	54.3μH
R_2	Ac resistance of transmitting coil	0.607Ω
L_3	Inductance of receiving coil	54.4μH
R_3	Ac resistance of receiving coil	0.612Ω
C_1	Parallel capacitance of MOSFET	4nF
C_2	Resonant capacitance of transmitting coil	476.5nF
C_3	Resonant capacitance of receiving coil	465.5pF
d	Transfer distance between transmitting and receiving coil	30cm

modules, after being able to receive the feedback, it enters into second stage to gradually increase the turn-on time of switch until it can receive the normal feedback. In Fig. 8(b), T_3 is working time of class-E inverter, T_4 is break time of class-E inverter, the Bluetooth module controls the class-E inverter to work intermittently.

V. EXPERIMENTAL RESULTS AND DISCUSSION

The experimental prototype of the WPT system is particularly shown in Fig. 10, and the parameters used in experiment circuits are listed in Table 1.

A. OUTPUT OF CLASS-E HIGH-FREQUENCY INVERTER

In Fig. 11, channel 1 represents gate driving voltage V_{Gate}. Channel 2 represents drain-source voltage V_{DS} of MOSFET. Channel 3 represents the voltage cross the load resistance V_L. It can be seen that the MOSFET of class-E high frequency inverter works in ZVS (zero voltage switching), and the
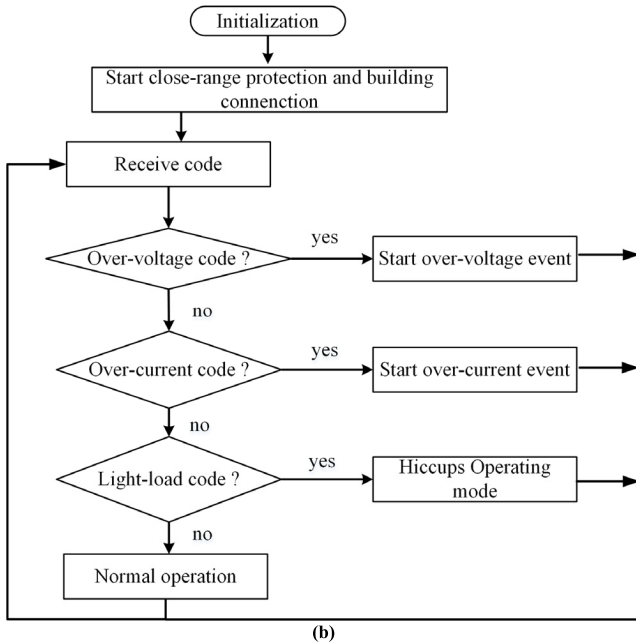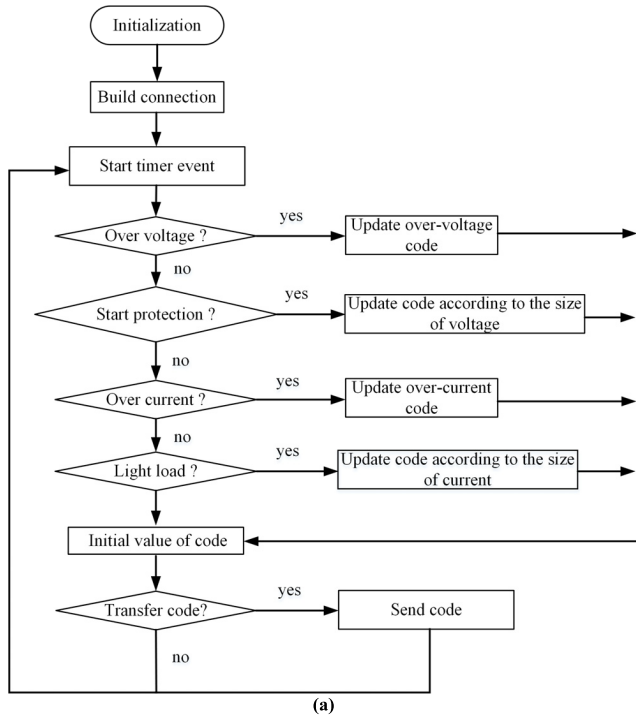
(a)

(b)

FIGURE 9. The control program flow chart of Bluetooth communication module. (a) The Bluetooth communication device in receiver. (b) The Bluetooth communication device in transmitter.

current flowing through transmitting coil has good sinusoidal properties.

B. ESULTS OF BLUETOOTH COMMUNICATION

The experimental waveforms of various protection functions based on Bluetooth communication are shown in Fig. 12. Channel 1 represents gate driving voltage signal of class-E
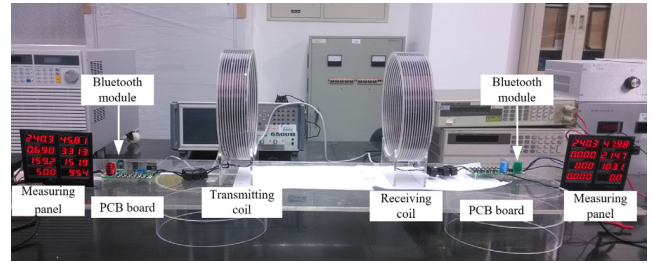

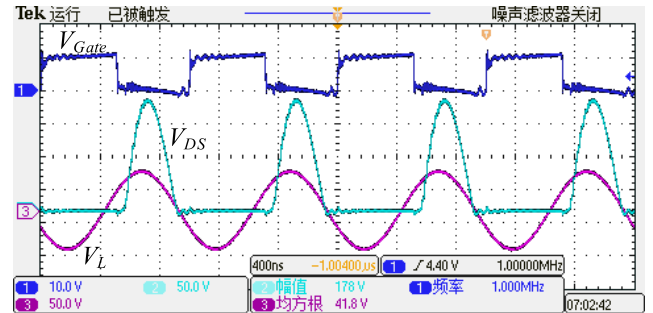**FIGURE 10.** The laboratory prototype of the WPT system.

FIGURE 11. Gate signal of S_1, drain-source voltage waveform of S_1 and voltage cross the load in the distance of 30cm.

TABLE 2. Power consumption of empty-load or light-load.

Symbol	Parameters		Values	
P_o	Output power	0W	5W	10W
P_{in} (no Bluetooth modules)	Input power	39.1W	42.5W	47.6W
P_{in} (no Bluetooth modules)	Input power	10.7W	21.2W	35.0W

inverter, channel 4 represents the input dc voltage of DC-DC converter on the receiver.

In Fig. 12(a), the function of overvoltage protection was well achieved, when the V_d exceeds the set value of 55V, the Bluetooth module on the receiver sends a high level to transmitter's Bluetooth module to stop driving class-E inverter, similarly, the principle of overcurrent protection is the same as it. But if there is no Bluetooth module, the V_d will keep increasing until the switch and PCB board are burnt out. In Fig. 12(b), class-E inverter enters into hiccup operating mode to achieve light-load protection according to the feedback from receiver's Bluetooth module when the load current is close to zero or the output power is less than 10W, the MOSFET works for 1.2ms, then stops for 2ms to 10ms, the stop time is determined by actual output power, and the measured light-load loss is shown in Table 2. From Table 2, it can be found that the light-load loss reduces greatly with Bluetooth communication. In Fig. 12(c), after the system has been launched, the working mode of close-distance protection is entered, the MOSFET works normally for 9ms, then stops working for 260ms, if the safe distance is
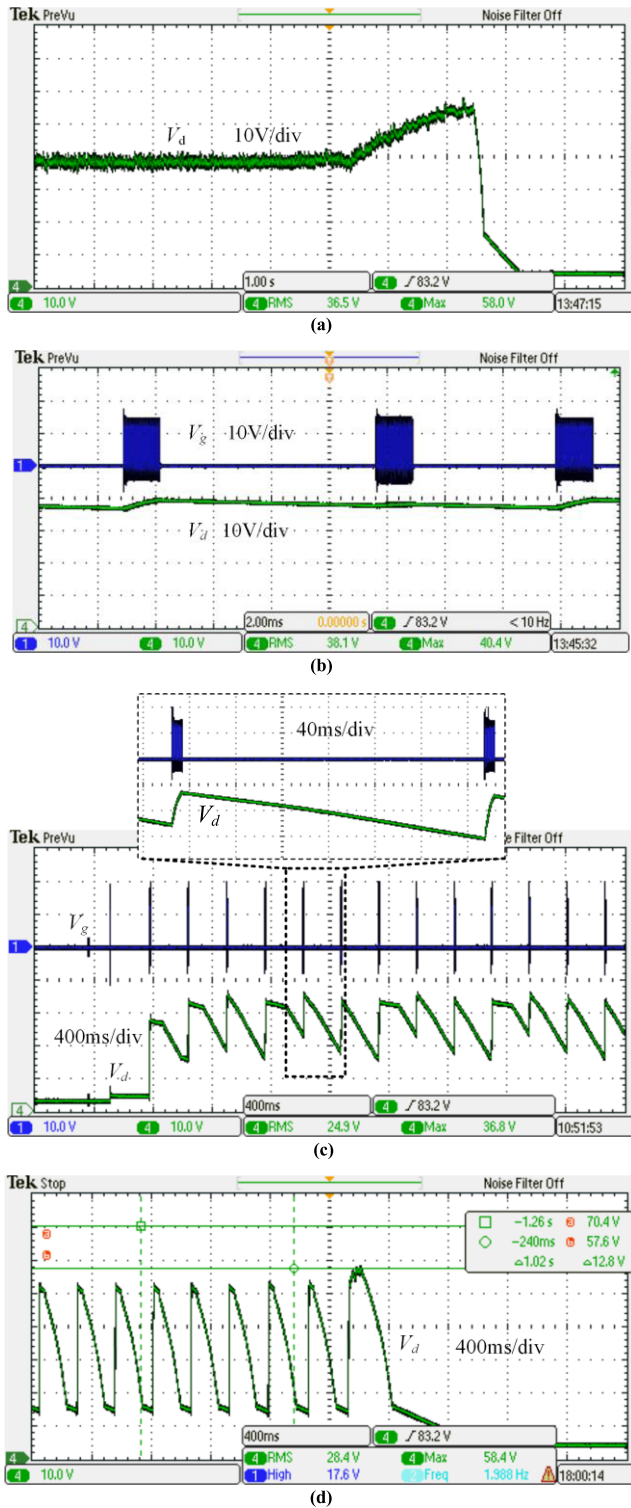
FIGURE 13. Output voltage and current waveforms of system. (a) Steady operation. (b) Startup process. (c) Sudden change of load.

C. OUTPUT POWER AND THE TOTAL EFFICIENCY

The static and dynamic waveforms of the experimental system are shown in Fig. 13, Channel 1 represents the output dc voltage of the system, channel 2 represents the output dc current of the system, channel 3 represents the output voltage ripple. And output power and efficiency curves of the whole experimental system from power-frequency input to dc output within a distance of 25cm to 45cm are shown in Fig. 14.

From Fig. 13, it can be noticed that the system has good reliability and stability. In Fig. 13(a), the output voltage is stable at 48V and its ripple is about 1%. In Fig. 13(b), the output voltage reached a stable value of 48V in 8ms when the system starts, the overshoot of voltage is only 3.6V. And in the situation that load sharply changes from rated value to zero, the system can be stabilized after 600us with 6.2V overshoot of voltage as shown in Fig. 13(c). Otherwise, output power and the total efficiency of system decrease with the increase of transfer distance, as shown in Fig. 14, it can be found that the experimental results are basically consistent with the theoretical analysis, which verifies the validity of the theoretical model. Moreover, within the transfer distance

FIGURE 12. Voltage waveforms. (a) Output dc voltage based on overvoltage protection. (b) Gate signal of class-E inverter and outputvoltage based on light-load protection. (c) Gate signal of class-E inverter and output voltage based on proximity protection. (d) Output dc voltage encountering with close distance in the process of starting up.

small during the startup process that makes the output voltage exceed the threshold, the Bluetooth module of transmitter continues to output low level to MOSFET to stop working, as shown in Fig. 12(d).
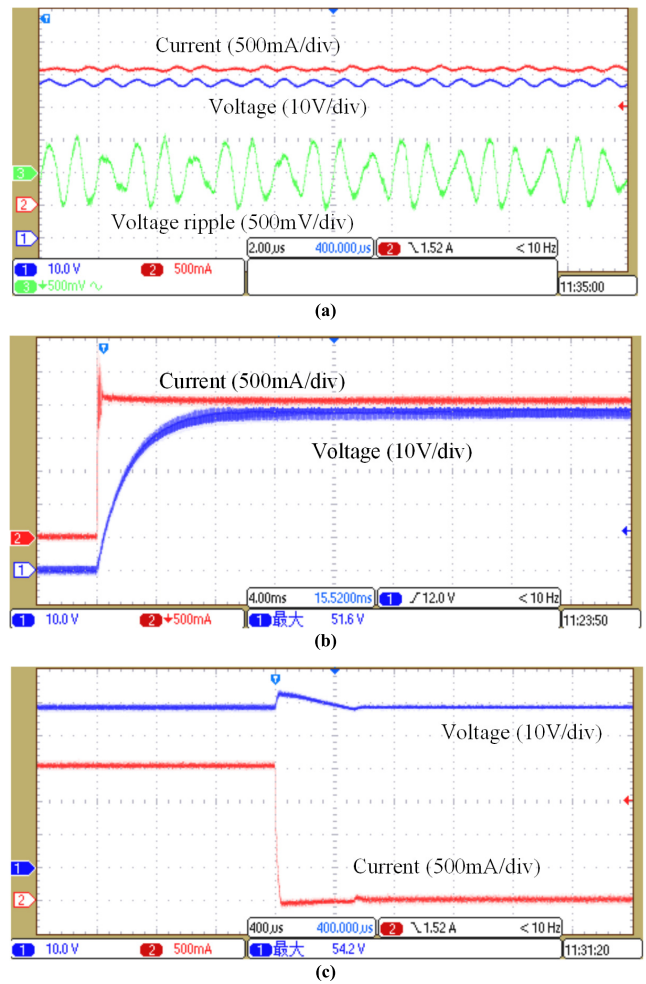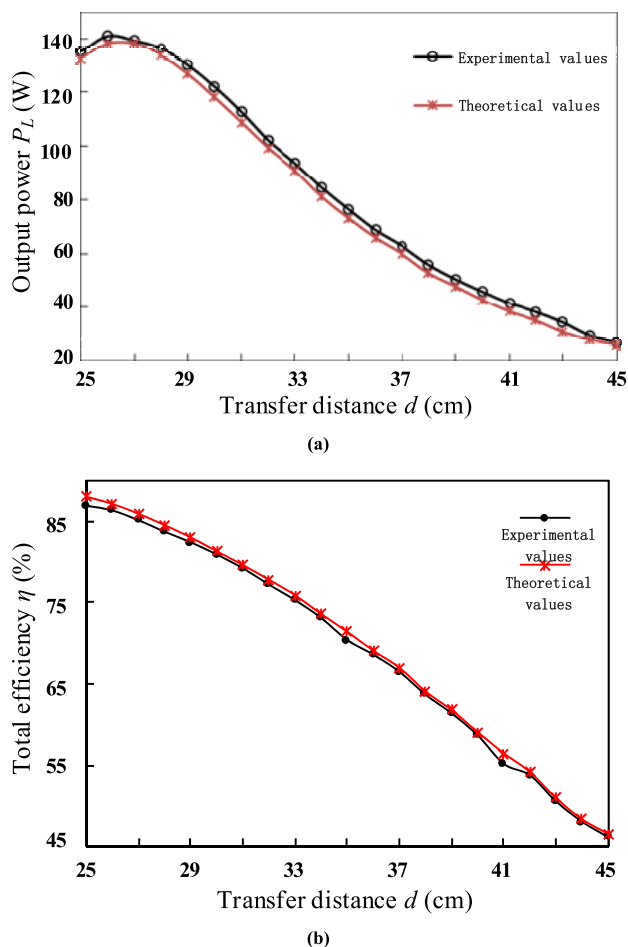
(a)

(b)

FIGURE 14. Output power and efficiency Voltage waveforms. (a) Output dc voltage based on overvoltage protection. (b) Gate signal of class-E inverter and output voltage based on light-load protection.

of 30cm, the output power is above 100W and the total efficiency is above 80%, which is enough to meet the power supply need of small household appliances.

VI. CONCLUSION

In this work, we presented a safe and reliable wireless power supply for small household appliances with high efficiency and stable output power. More specifically, a novel energy model was proposed to analyze the energy exchange process between the transmitting and receiving coil, and characteristics of output power and transfer efficiency of WPT system. Furthermore, the Bluetooth communication was used to provide various protection functions to the system, including light load, overvoltage, overcurrent and close distance, which ensures the system operates safety and stably. Finally, a wireless power supply for small household appliances with a stable output dc voltage of 48V, a large output power of 100W, and a high total efficiency of more than 80% within a distance of 30cm, was designed and implemented. And the experimental results also verified the effectiveness of the theoretical model.

REFERENCES

[1] (Apr. 22, 2017). *Most Common Causes of Electrical Accident in the Home*. [Online]. Available: https://brayelectricalservices.com/650-2/

[2] S. Benanti *et al.*, "Wireless power transmission for house appliances: A small-scale resonant coupling prototype," in *Proc. AEIT Int. Annu. Conf. (AEIT)*, Capri, Italy, Oct. 2016, pp. 1–6, doi: 10.23919/AEIT.2016.7892812.

[3] J. Salton. (Sep. 30, 2009). *Dell's Latitude Z: World's First Laptop With Wireless Docking and Inductive Charging*. [Online]. Available: https://newatlas.com/dells-latitude-z-irst-laptop-wireless-docking-inductive-charging/12979/

[4] R. Larsen. (Sep. 10, 2010). *Haier Demonstrates TV With Wireless Power*. [Online]. Available: https://www.flatpanelshd.com/news.php?subaction=showfull&id=1284118520

[5] D. Xiaodan. (Jan. 9, 2010). *Chinese Companies Unveil Innovations at 2010 CES in Las Vegas*. [Online]. Available: http://english.cctv.com/20100109/102376.shtml

[6] (Aug. 14, 2015). *Haier Unveils the Future of Household Appliances at IFA 2012*. [Online]. Available: http://www.haier.com/uk/newspress/pressreleases/news2012/201508/t2015081_281359.shtml

[7] Garima. (Mar. 12, 2013). *Transparent and Wireless-Powered OLED Lighting Panels by Toshiba*. [Online]. Available: http://www.homecrux.com/transparent-and-wireless-powered-oled-lighting-panels-by-toshiba/4546/

[8] D. T. Nguyen, E. S. Lee, B. G. Choi, and C. T. Rim, "Optimal shaped dipole-coil design and experimental verification of inductive power transfer system for home applications," in *Proc. IEEE Appl. Power Electron. Conf. Exposit. (APEC)*, Long Beach, CA, USA, Mar. 2016, pp. 1773–1779, doi: 10.1109/APEC.2016.7468108.

[9] J. Kim, D.-H. Kim, and Y.-J. Park, "Effective magnetic resonant wireless power transfer system over medium range using an intermediate resonant coil of two loops," in *Proc. IEEE-APS Top. Conf. Antennas Propag. Wireless Commun. (APWC)*, Turin, Italy, Sep. 2015, pp. 502–505, doi: 10.1109/APWC.2015.7300166.

[10] J. Kim, H.-C. Son, D.-H. Kim, and Y.-J. Park, "Optimal design of a wireless power transfer system with multiple self-resonators for an LED TV," *IEEE Trans. Consum. Electron.*, vol. 58, no. 3, pp. 775–780, Aug. 2012.

[11] A. Kurs, A. Karalis, R. Moffatt, J. D. Joannopoulos, P. Fisher, and M. Soljačić, "Wireless power transfer via strongly coupled magnetic resonances," *Science*, vol. 317, no. 5834, pp. 83–86, 2007.

[12] B. H. Waters, B. J. Mahoney, G. Lee, and J. R. Smith, "Optimal coil size ratios for wireless power transfer applications," in *Proc. IEEE ISCAS*, Jun. 2014, pp. 2045–2048, doi: 10/1109/ISCAS.2014.6865567.

[13] F. Corti, F. Grasso, A. Reatti, A. Ayachit, D. K. Saini, and M. K. Kazimierczuk, "Design of class-E ZVS inverter with loosely-coupled transformer at fixed coupling coefficient," in *Proc. IEEE IECON*, Oct. 2016, pp. 5627–5632, doi: 10/1109/IECON.2016.7793285.

[14] X. Zhang, X. Zhang, Y. Yao, H. Yang, Y. Wang, and D. Xu, "High-efficiency magnetic coupling resonant wireless power transfer system with class-e amplifier and class-e rectifierr," in *Proc. IEEE ITEC*, Aug. 2017, pp. 1–5, doi: 10/1109/ITEC-AP.2017.8080933.
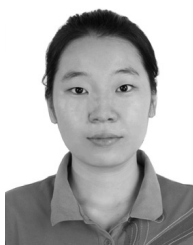
XUJIAN SHU was born in Anqing, Anhui, China, in 1993. She received the B.S. degree in electrical engineering from the China University of Mining and Technology, Xuzhou, China, in 2011. She is currently pursuing the Ph.D. degree in power electronics with the School of Electric Power, South China University of Technology, Guangzhou, China.

Her research interests include wireless power transfer applications and fractional-order systems.

WENXUN XIAO (M'14) was born in Danzhou, Hainan, China, in 1979. He received the B.S. degree in electrical engineering and automation and the M.S. and Ph.D. degrees in power electronics and power drives from the South China University of Technology, Guangzhou, China, in 2002, 2005, and 2008, respectively.

Since 2008, he has been with the School of Electrical Power, South China University of Technology, where he is currently an Associate Professor. His research interests include topologies and control methods of power electronics, wireless power transmission technology, renewable energy technologies, and microgrids.

BO ZHANG (M'03–SM'15) was born in Shanghai, China, in 1962. He received the B.S. degree in electrical engineering from Zhejiang University, Hangzhou, China, in 1982, the M.S. degree in power electronics from Southwest Jiaotong University, Chengdu, China, in 1988, and the Ph.D. degree in power electronics from the Nanjing University of Aeronautics and Astronautics, Nanjing, China, in 1994.

He is currently a Professor with the School of Electric Power, South China University of Technology, Guangzhou, China. He has authored or co-authored four books in IEEE–Wiley and Springer and over 450 technical papers, and he holds 100 patents. His current research interests include nonlinear analysis, modeling and control of power electronic converters, and wireless power transfer applications.

● ● ●